ACS Macro Letters

Letter

pubs.acs.org/macroletters

Synthesis of Polymer Electrolytes Based on Poly(ethylene oxide) and an Anion-Stabilizing Hard Polymer for Enhancing Conductivity and Cation Transport

Gyuha Jo,[†] Hongchan Jeon,[†] and Moon Jeong Park*[,†,‡]

[†]Department of Chemistry and [‡]Division of Advanced Materials Science, Pohang University of Science and Technology (POSTECH), Pohang, Korea 790-784

Supporting Information

ABSTRACT: We have investigated a new methodology for improving the ionic conductivity and cation transport of polymer electrolytes by incorporating an anion-stabilizing hard polymer. A lamellar-forming poly(ethylene oxide-*b*-dithiooxamide) (PEO-*b*-PDTOA) block copolymer having enhanced ion conduction and mechanical strength, arising from PEO and PDTOA, respectively, was synthesized. Compared to a simple PEO/PDTOA blend, lithium salt-doped PEO-*b*-PDTOA exhibited significantly enhanced ionic conductivity, which is ascribed to efficient ion transport along the nanoscale PEO domains. Strikingly, by applying a dc polarization voltage, the inclusion of PDTOA afforded a high ratio of the steady state to the initial current flow of 0.67 for the PEO-*b*-PDTOA electrolytes, surpassing the value of 0.31 observed for conventional PEO-salt electrolytes. A key reason for achieving enhanced cation transport was the hydrogen bonding interactions between the thioamide moieties of PDTOA and the anions of lithium salts. This work provides fascinating experimental insights into the enhancement of cation transport of polymer electrolytes without chemically bonded negative charges and has implications for fast charging energy storage systems.

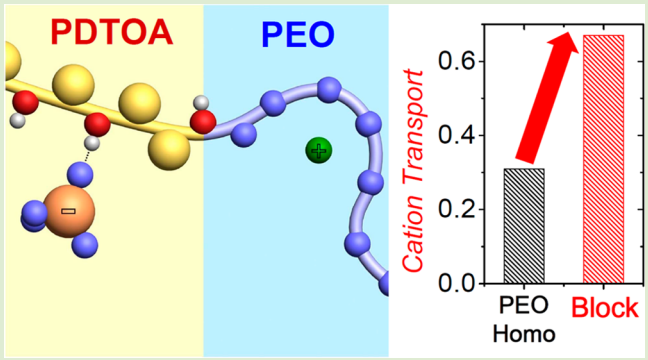

Recently, global warming and fossil fuel deficiency have increased the needs for developing new energy storage systems (ESSs) that are environmentally benign and possess high efficiencies.[1−4] Lithium ion batteries (LIBs) have been touted as the most promising candidates, owing to their unique advantages, such as long cycle life,[5,6] high specific capacity,[7−9] and high cell potential.[10] One major drawback of conventional LIBs is that the cells contain flammable liquid electrolytes, leading to inherent safety issues.[8,11] This has led to the development of lithium polymer batteries, where the use of liquid electrolytes is eliminated. The most widely employed polymer electrolytes for lithium polymer batteries are the poly(ethylene oxide) (PEO)−lithium salt complexes, which possess advantages such as high ionic conductivity and low volatility.[12,13] However, owing to the poor mechanical properties of PEO, there is an inevitable need for an additional polymeric separator, to avoid short-circuiting the battery and to impede lithium dendrite formation.[14,15]

In order to improve the mechanical properties of PEO, various types of PEO-based polymers combined with mechanically robust polymer chains have been investigated.[16−27] Among such materials, block copolymers, in which hard polymers and PEO are covalently attached, are attractive. These block copolymers have a synergistic combination of mechanical strength and lithium ion conduction arising from the hard polymer and PEO, respectively.[16,19−27] An example of a typical hard polymer is polystyrene (PS), which has a high Young's modulus of 3 GPa and a high glass transition temperature (T_g) of around 100 °C.[17,19−26] In the PS-*b*-PEO block copolymer, PS exhibits hydrophobic characteristics leading to strongly segregated PS and PEO phases in the nanometer scale, which allows the structural integrity to be maintained by effectively confining the lithium salt within the PEO domains.[19,28] This has motivated researchers to study the relationship between the nanostructure and conductivity of lithium salt-doped PS-*b*-PEO block copolymers and a variety of observations concerning the morphology effects have been reported.[21,22] Recent work by Balsara and co-workers has further elucidated the effect of T_g[24] and crystallinity[27] of the constituent hard polymer on ion conduction in PEO, revealing new means for achieving the desired ion transport properties using PEO-containing block copolymer electrolytes.

Unfortunately, polymer−lithium salt complexes have exhibited immense shortcomings due to concentration polarization, which is ascribed to the motion of free anions within PEO.[29,30] The effects of concentration polarization limit the charge/discharge rates of lithium batteries and lead to the back diffusion of salt concentration gradients.[29,30] In light of such

Received: November 11, 2014
Accepted: January 21, 2015
Published: January 26, 2015

DOI: 10.1021/mz500717j
ACS Macro Lett. 2015, 4, 225−230

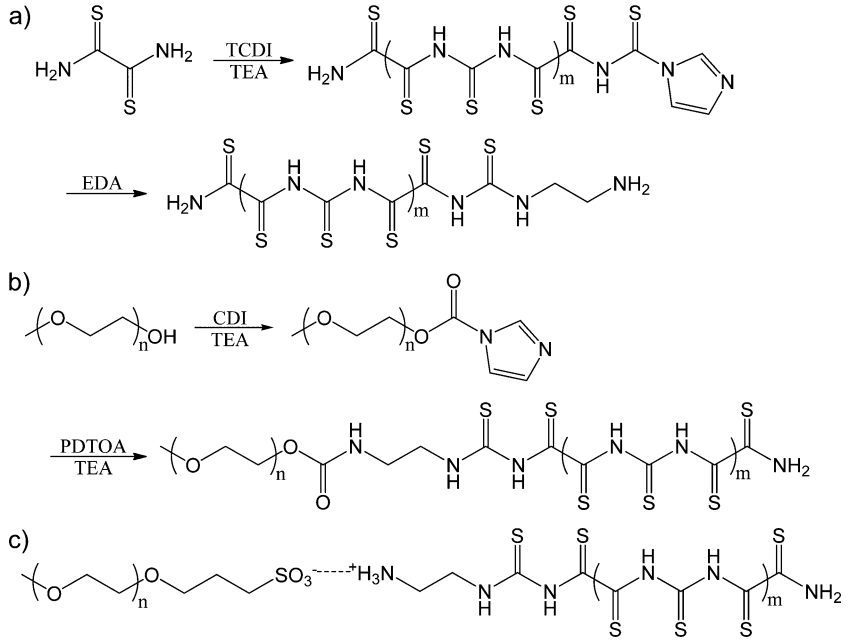

Figure 1. Synthetic procedures of (a) PDTOA homopolymer, (b) PEO-*b*-PDTOA block copolymer (**block**), and (c) PEOS/PDTOA charged blend (**C-blend**).

discoveries, polymers tethered to anionic moieties have recently received great attention[31−35] and have been prominently featured as single ion conductors with high lithium ion transference numbers of up to 0.95.[35] Examples of such polymers include alternating copolymers comprised of PEO and sulfoisophthalate,[31] graft copolymers composed of polysiloxane backbone and borate side chains,[32] and block copolymers in which PEO and poly(styrene trifluoromethane sulfonylimide) are covalently attached.[33−35] While the use of single ion conductors opens a new chapter in the polymer electrolyte technology, achieving high ionic conductivities of over 10^{-4} S/cm remains a challenging task.[31−35] This is ascribed to the limited polymer chain motions due to the chemically fixed negative charges.

Here, we report a new type of polymer electrolyte comprised of PEO and poly(dithiooxamide) (PDTOA) chains, which exhibits high ionic conductivity and improved cation transport. The high T_g of PDTOA (130 °C; Figure S1, Supporting Information) can be the additional advantage to improve mechanical stability at elevated temperatures. In addition, the presence of the thioamide group in PDTOA serves to reduce the anion diffusion rate via hydrogen bonding interactions with the anion of the lithium salt. The results described herein are likely to offer future research avenues for achieving improved ionic conductivity and cation transport of polymer electrolytes, for applications in emerging energy storage technologies.

Figure 1a describes the synthesis of PDTOA homopolymer using dithiooxamide (DTOA), 1,1′-thiocarbonyldiimidazole (TCDI), and triethylamine (TEA) as monomer, linker, and catalyst, respectively. The residual imidazole terminal moiety of PDTOA was converted to an amine group via further reaction with excess ethylenediamine (EDA). The molecular weight of the synthesized PDTOA was determined to be 6.5 kg/mol, by end-group analysis using ^{1}H NMR spectroscopy in DMF-d_7. Next, the PEO-*b*-PDTOA block copolymer was synthesized by reacting carbonyldiimidazole-capped poly(ethylene glycol) methyl ether (MPEO-CDI, 5 kg/mol) with PDTOA, as shown in Figure 1b. The molecular characteristics of the synthesized PEO-*b*-PDTOA (5−6.5 kg/mol) were confirmed by ^{1}H NMR spectroscopy in the mixture of DMF-d_7 and $CDCl_3$. PEO-*b*-PDTOA will be referred to as **block**, hereafter. Representative ^{1}H NMR spectra of PDTOA, MPEO-CDI, and **block** are shown in Figure S2, Supporting Information.

As an alternative method, an end-linked polymer resembling a block copolymer was prepared by synthesizing MPEO with a sulfonate terminal group (PEOS; ^{1}H NMR spectrum of PEOS is given in Figure S3). Blending PEOS (anionic polymer) with PDTOA (cationic polymer) using a polar solvent was expected to result in the formation of a blocky PEOS/PDTOA charged blend (referred to as **C-blend**) via electrostatic attractions, as depicted in Figure 1c. The blend of unmodified PEO and PDTOA (referred to as **blend**) was used as control.

The microphase separation properties of **block**, **C-blend**, and **blend** samples were investigated using small-angle X-ray scattering (SAXS) experiments. Representative scattering profiles of the samples acquired at room temperature are shown in Figure 2a, which were unchanged in the temperature window of our interest. In the case of the **block** sample, a series of Bragg peaks at $1q^*$, $2q^*$, $3q^*$, $4q^*$, and $5q^*$, with $q^* = 2\pi/d_{100}$ (d_{100} is the domain size, which was 33.7 nm for **block**), were observed, as noted by inverted filled triangles (▼), indicating the presence of well-defined lamellar morphology. Interestingly, the **C-blend** sample also exhibited Bragg peaks at $1q^*$, $2q^*$, and $3q^*$, as marked by inverted open triangles (▽), with d_{100} of 24 nm. In contrast, the scattering profile of the **blend** sample was featureless. Although the scattering profile for the **C-blend** sample was poorly resolved, nanoscale−phase separation into a lamellar structure can be expected through effective Coulombic interactions between PEOS and PDTOA chain in contrast with the **blend** sample. The origin of large deviations in the domain sizes of **block** and **C-blend** may be complicated by several factors, such as dissimilar segregation strength between PDTOA and PEO phases for **block** and **C-blend** and the participation of a limited number of PDTOA and PEOS chains in self-assembly, in the case of **C-blend**.

DOI: 10.1021/mz500717j
ACS Macro Lett. 2015, 4, 225−230

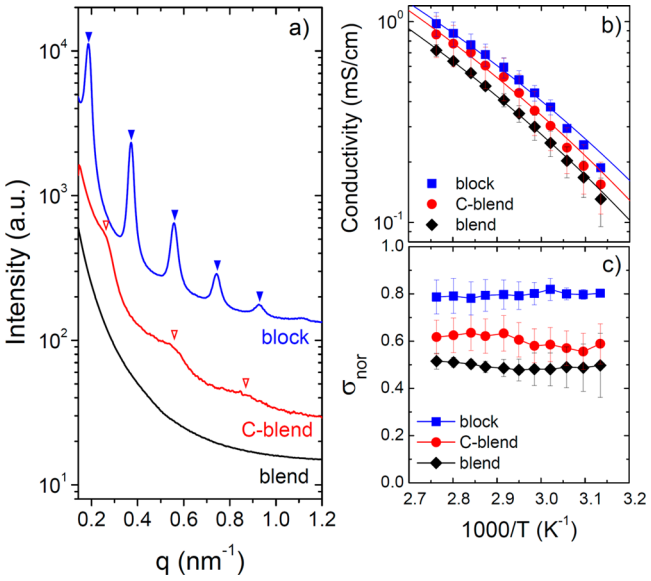

Figure 2. (a) Scattering profiles of **block**, **C-blend**, and **blend** samples measured at room temperature. (b) The temperature-dependent ionic conductivity of each sample at r = 0.06 (r = [Li]/[EO]). Solid lines indicate analysis using VTF equation. (c) Normalized conductivity (σ_{nor}) of each sample using eq 1

Note in passing that the well-defined lamellar morphology of **block** was preserved upon the addition of lithium salt, although the domain size and segregation strength were gradually reduced with the increase in the amount of salt (data not shown here).

The ionic conductivities of the **block**, **C-blend**, and **blend** samples containing PEO fractions of 43, 50, and 50 wt %, respectively, were investigated next. Figure 2b presents the representative data obtained in the temperature range 45−90 °C at a lithium bis(trifluoromethane sulfonyl) imide (LiTFSI) doping ratio (r, [Li]/[EO]) of 0.06. **Blend** sample, which lacks organization, exhibited the lowest ionic conductivities of 1.3 × 10^{-4} S/cm and 7.0 × 10^{-4} S/cm at 45 and 90 °C, respectively. On the other hand, the **block** sample showed improved ionic conductivity values of 2 × 10^{-4} S/cm and 1 × 10^{-3} S/cm at 45 and 90 °C, respectively. Interestingly, the ionic conductivity of the **C-blend** sample was 30% higher than the **blend** sample, in the entire temperature window. This is inconsistent with the conductivities of PEOS and PEO homopolymers because PEOS showed approximately 40% lower conductivity than PEO as a result of end-substitution (Figure S4, Supporting Information).[22] This result demonstrates the role played by microphase separation in improving the ion transport efficiency of the **block** and **C-blend** samples by facilitating fast ion transfer along confined, less tortuous PEO domains. Solid lines in Figure 2b represent the analysis using Vogel−Tamman−Fulcher (VTF) equation, which was performed to identify potential barriers to ion conduction in different samples.[36] The activation energies (E_a) for **block**, **C-blend**, and **blend** were determined to be 7.89, 8.41, and 8.48 kJ/mol, respectively.

The relationship between nanoscale morphology and ion transport properties was further elucidated by normalizing the conductivity data (Figure 2b) based on the conductivity of the PEO homopolymer (Figure S4). We employed eq 1 given below,[37] where σ_{nor} is the normalized conductivity, σ_{sample} is the conductivity of the LiTFSI-doped samples, and σ_{homo} is that of the homopolymer analog measured using 5 kg/mol PEO at a given LiTFSI concentration. The ϕ_{PEO} was estimated on the density of DTOA monomer (1.523 g/cm^3) and that of amorphous PEO chains (1.123 g/cm^3).

$$\sigma_{nor} = \frac{\sigma_{sample}}{\phi_{PEO}\sigma_{homo}} \quad (1)$$

Figure 2c shows the σ_{nor} values for **block**, **C-blend**, and **blend** in a temperature window of 45−90 °C at r = 0.06. Strikingly, the σ_{nor} values of the structured samples (**block** and **C-blend**) were higher than that of the **blend** sample. σ_{nor} for the three types of samples is ranked in the order of **block** > **C-blend** > **blend**, which implies that well-defined phase boundaries between PDTOA and PEO are important for enhancing the Li$^+$-ion transport efficiency. It is particularly noteworthy that the σ_{nor} value of 0.8 for **block**, surpassed the theoretical value of 0.66, which is calculated for polymers possessing randomly organized lamellar grains.[37] It is also worth noting that while **blend** has the lowest σ_{nor} of 0.5 among the three samples in this study, the value itself is not small compared to the value reported for conventional PEO-based polymer electrolytes in the literature. For example, PS−PEO block copolymers with comparable PEO molecular weights have shown σ_{nor} values in the range of 0.05−0.2.[22,24]

To elucidate the mechanisms behind the improved ion transport properties of polymer electrolytes containing PDTOA, the efficacy of Li$^+$-ion transport of each sample was quantified by electrode polarization experiments at 70 °C and a polarization voltage (ΔV) of 0.1 V using two Li metal electrodes. All sample preparation and measurements were performed inside a high-purity Ar-filled glovebox to avoid any possible contamination by moisture and oxygen. Figure 3a shows a representative current profile obtained during

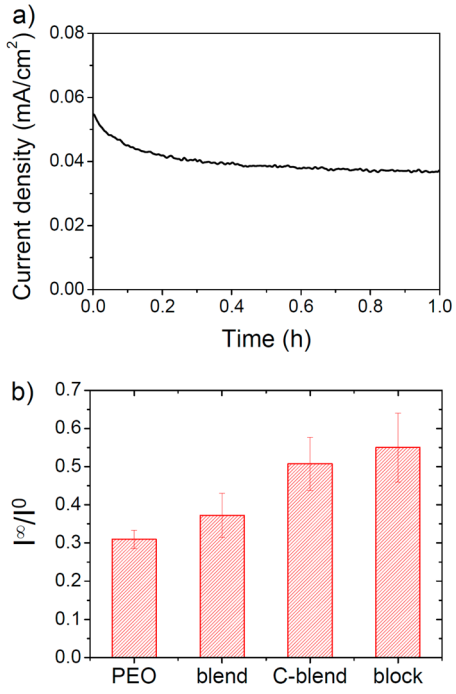

Figure 3. (a) Representative electrode polarization test profile of **block** at r = 0.03, T = 70 °C, and ΔV = 0.1. (b) The average ratios of the steady state to the initial current flow of **blend**, **C-blend**, and **block**, compared to that of PEO, obtained with different salt concentrations (r = 0.03, 0.04, 0.06, 0.08).

DOI: 10.1021/mz500717j
ACS Macro Lett. 2015, 4, 225−230

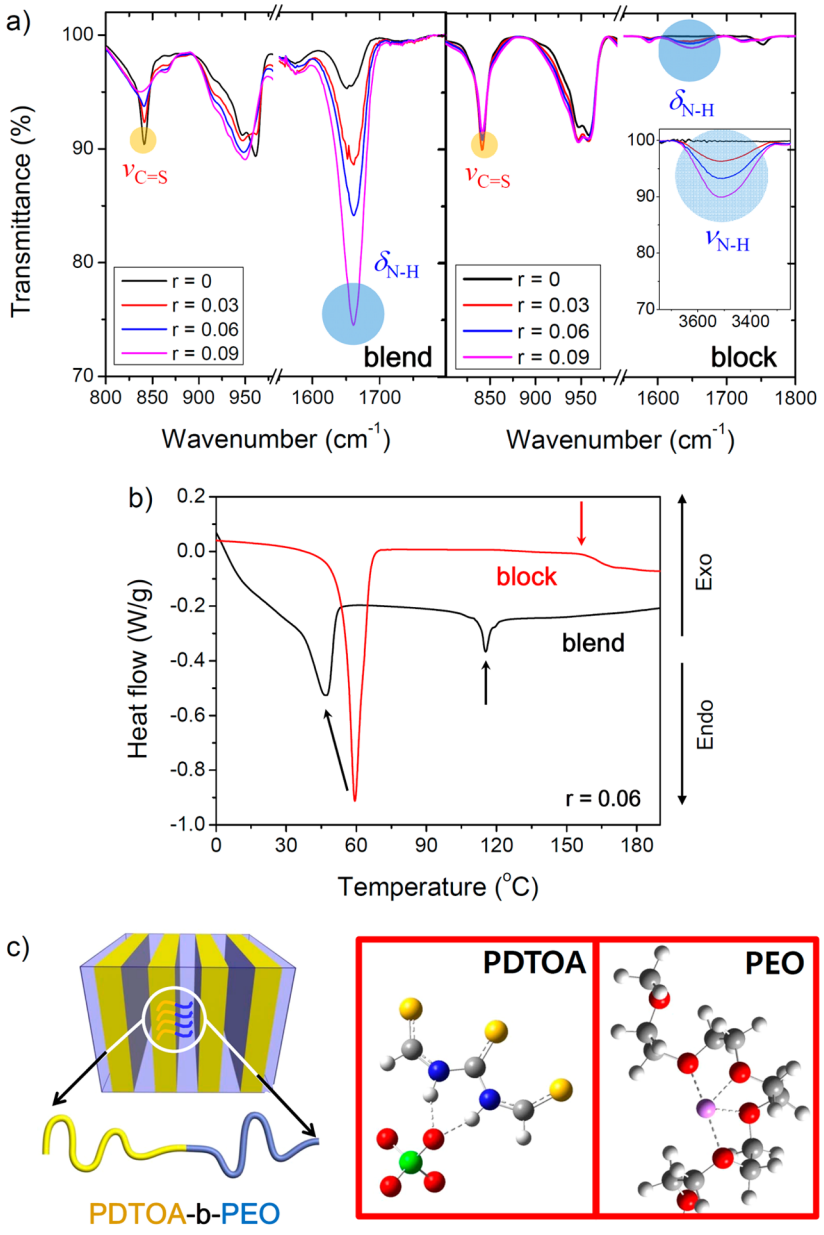

Figure 4. (a) FT-IR spectra of **blend** and **block** showing two characteristic peaks of $\nu_{C=S}$ and δ_{N-H} at 840 and 1650 cm^{-1}, respectively, at different lithium salt doping levels. Inset figure shows the IR absorptions associated with N−H vibration for **block**. (b) DSC thermograms of **block** and **blend** at r = 0.06. (c) Schematic drawings of the proposed molecular interactions in lithium salt-doped **block**.

polarization of **block** at r = 0.03 for 1 h. The ratio of the steady-state to the initial current flow (I^{∞}/I^{0}) was monitored during the polarization experiments and intriguingly, the high I^{∞}/I^{0} of 0.67 was determined for **block**, which far exceeds the low values (ca. 0.30) of conventional PEO−lithium salt complexes reported in the literature.[38−40] This implies that much of the current in **block** is carried by the cation.[40]

Figure 3b shows the average I^{∞}/I^{0} values of **block**, **C-blend**, and **blend**, compared to that of PEO homopolymer, obtained with different salt concentrations (r = 0.3, 0.4, 0.6, 0.8). The **block** samples exhibited the highest I^{∞}/I^{0} values, whereas the **blend** samples exhibited the lowest I^{∞}/I^{0} values among **block**, **C-blend**, and **blend**. Considering that **C-blend** also exhibited improved I^{∞}/I^{0} values, we deduce that the thioamide moieties of microphase-separated PDTOA serve to reduce anion diffusion through effective hydrogen-bonding interactions.

In order to demonstrate the hypothesis concerning the role of the thioamide moieties of microphase-separated PDTOA in stabilizing anion of lithium salt, we carried out a set of quantitative investigation. First, four possible molecular interactions, (1) N−H (PDTOA) interaction with the anion, (2) Li^{+} interaction with C═S (PDTOA), (3) Li^{+} interaction with the anion, and (4) N−H (PDTOA) interaction with PEO, were analyzed by combining DFT calculations (ab initio calculations at 0 K in a vacuum using a DFT exchange-correlation functional, B3LYP, with 6-31G(d) basis set) and Fourier transform infrared (FT-IR) spectroscopy experiments. Since IR absorption peaks of TFSI anion overlap with those of PDTOA, $LiClO_4$ was employed for these studies, under the assumption that the use of $LiClO_4$ would not significantly alter the salt dissociation behavior. The hydrogen bonding interaction between N−H of PDTOA and ClO_4^{-} was determined to be 51.6 kcal/mol and the binding energy of

DOI: 10.1021/mz500717j
ACS Macro Lett. 2015, 4, 225−230

Li^+ and C═S of PDTOA was calculated as 43.5 kcal/mol. The largest binding energy of 160.3 kcal/mol was predicted for Li^+ and ClO_4^-; however, the high degree of dissociation of $LiClO_4$ in **block** (>90%, Figure S5, Supporting Information) led us to disregard the charge−charge interaction. The hydrogen bonding interaction between N−H (PDTOA) and PEO was as weak as 1.6 kcal/mol. Coupling schemes at optimized geometries are presented in Figure S6.

N−H interaction with the anion (or with ether oxygen) and C═S interaction with Li^+ were further analyzed experimentally. Representative FT-IR spectra of **blend** and **block**, measured at different salt concentrations, are shown in Figure 4a. Two characteristic peaks of $\nu_{C=S}$ and δ_{N-H} were observed at 840 and 1650 cm^{-1}, respectively. Without addition of lithium salt to **blend** and **block**, the IR absorptions associated with C═S vibration were similar, but the increasing amount of lithium salt caused a substantial reduction in the peak intensity and shift of the peak toward lower frequencies for **blend**, as opposed to nonsignificant changes in C═S vibrational motion of **block**. The negligible C═S interaction with Li^+ for **block** implies that most of the Li^+-ion coordinates with ether oxygen of microphase-separated PEO domains, whereas the extensive interaction between Li^+ and C═S of PDTOA in **blend** (which diminishes the double-bond character of the C═S bond) is ascribed to the phase mixing between PEO and PDTOA. The same analogy can be applied to the changes in N−H bending motion. With increasing lithium salt concentration, small but noticeable increases in δ_{N-H} and ν_{N-H} (at around 3500 cm^{-1}, see inset) were observed for **block**, attributed to the N−H interaction with the anion. In contrast, the largely increased IR absorptions of δ_{N-H} for **blend** were evident owing to the phase mixing between PDTOA and PEO, driven by hydrogen bonding interaction.

Next, differential scanning calorimetry (DSC) experiments were performed and representative DSC thermograms of LiTFSI-doped **block** and **blend** are given in Figure 4b, representing markedly different thermal transitions of two samples. A small heat of melting at low temperature was observed for PEO phases of LiTFSI-doped **blend**, compared to highly crystalline characteristics of PEO in LiTFSI-doped **block**. This indicates that lithium salt (particularly, unbound anion) has a plasticizing effect on the PEO phases of **blend**. A new melting point (T_m) at 115 °C was observed only for the **blend**, signaling the appearance of crystalline characteristics in PDTOA under the influence of the phase mixing between PEO and PDTOA. The T_g of PDTOA of LiTFSI-doped **block** was raised by 27 °C at r = 0.06, which can serve as evidence of the anion interaction with PDTOA chains. The T_g of PDTOA of LiTFSI-doped **blend** was invisible, presumably, overshadowed by T_m in a similar temperature range.

The molecular interactions that occur in lithium salt-doped **block** are schematically depicted in Figure 4c. Most of the Li^+-ion coordinates with ether oxygen of microphase-separated PEO, whereas the anion is stabilized in the PDTOA phases via hydrogen bonding interactions. This should be responsible for the improved ion transport properties of our new block copolymer electrolytes.

In summary, we have demonstrated the role of the constituent hard polymer in enhancing ion transport properties of lithium salt-polymer complexes by synthesizing new polymer electrolytes comprised of PEO and PDTOA chains. By designing the polymers as block or end-linked charged blends, well-organized or quasi-ordered lamellar morphology was successfully created, which proved beneficial in increasing the ion transport rates. In particular, our results show that the unique anion-stabilizing ability of thioamide-containing PDTOA chains plays an important role in improving the cation transport, which is attributed to the specific hydrogen bonding interactions with the anion of the lithium salt. The unprecedented, neighboring polymer-driven improvement in the ion transport properties of PEO-based polymer electrolytes established in the present study can aid the development of future research strategies for designing polymer electrolytes with enhanced performances.

■ ASSOCIATED CONTENT

Ⓢ Supporting Information

Additional information on the synthesis and characterization of PDTOA, MPEO-CDI, PEOS homopolymers, and PEO-*b*-PDTOA block copolymer. This material is available free of charge via the Internet at http://pubs.acs.org.

■ AUTHOR INFORMATION

Corresponding Author

*E-mail: moonpark@postech.edu.

Notes

The authors declare no competing financial interest.

■ ACKNOWLEDGMENTS

This work was financially supported by National Nuclear R&D Program (2011-0031931) and the Global Frontier R&D program on Center for Multiscale Energy System funded by the National Research Foundation under the Ministry of Science, ICT & Future, Korea.

■ REFERENCES

(1) Arico, A. S.; Bruce, P. G.; Scrosati, B.; Tarascon, J.; Schalkwijk, W. V. *Nat. Mater.* **2005**, *4*, 366−377.
(2) Armand, M.; Tarascon, J. *Nature* **2008**, *451*, 652−657.
(3) Kim, S. W.; Seo, D. H.; Ma, X. H.; Ceder, G.; Kang, K. *Adv. Energy Mater.* **2012**, *2*, 710−721.
(4) Dunn, B.; Kamath, H.; Tarascon, J.-M. *Science* **2011**, *334*, 928−935.
(5) Wu, H.; Chan, G.; Choi, J. W.; Ryu, I.; Yao, Y.; McDowell, M. T.; Lee, S. W.; Jackson, A.; Yang, Y.; Hu, L.; Cui, Y. *Nat. Nanotechnol.* **2012**, *7*, 310−315.
(6) Wang, Z. L.; Xu, D.; Wang, H. G.; Wu, Z.; Zhang, X. B. *ACS Nano* **2013**, *7*, 2422−2430.
(7) Wang, W.; Kumta, P. N. *ACS Nano* **2010**, *3*, 2233−2241.
(8) Jo, G.; Choi, I.; Ahn, H.; Park, M. J. *Chem. Commun.* **2012**, *48*, 3987−3989.
(9) Simmonds, A. G.; Griebel, J. J.; Park, J.; Kim, K. R.; Chung, W. J.; Oleshko, V. P.; Kim, J.; Kim, E. T.; Glass, R. S.; Soles, C. L.; Sung, Y.-E.; Char, K.; Pyun, J. *ACS Macro Lett.* **2014**, *3*, 229−232.
(10) Tarascon, J. M.; Armand, M. *Nature* **2001**, *414*, 359−367.
(11) Scrosati, B.; Garche, J. *J. Power Sources* **2010**, *195*, 2419−2430.
(12) Michael, M. S.; Jacob, M. M. E.; Prabaharan, S. R. S.; Radhakrishna, S. *Solid State Ionics* **1997**, *98*, 167−174.
(13) Scrosati, B.; Croce, F.; Panero, S. *J. Power Sources* **2001**, *100*, 93−100.
(14) Rosso, M.; Brissot, C.; Teyssot, A.; Dolle, M.; Sannier, L.; Tarascon, J. M.; Bouchetc, R.; Lascaud, S. *Electrochim. Acta* **2006**, *51*, 5334−5340.
(15) Harry, K. J.; Hallinan, D. T.; Parkinson, D. Y.; MacDowell, A. A.; Balsara, N. P. *Nat. Mater.* **2014**, *13*, 69−73.
(16) Choi, I.; Ahn, H.; Park, M. J. *Macromolecules* **2011**, *44*, 7327−7334.

DOI: 10.1021/mz500717j
ACS Macro Lett. 2015, 4, 225−230

(17) Wang, C. X.; Sakai, T.; Watanabe, O.; Hirahara, K.; Nakanishi, T. J. *Electrochem. Soc.* **2003**, *150*, A1166−A1170.
(18) Yuan, F.; Chen, H. Z.; Yang, H. Y.; Li, H. Y.; Wang, M. *Mater. Chem. Phys.* **2005**, *89*, 390−394.
(19) Singh, M.; Odusanya, O.; Wilmes, G. M.; Eitouni, H. B.; Gomez, E. D.; Patel, A. J.; Chen, V. L.; Park, M. J.; Fragouli, P.; Iatrou, H.; Hadjichristidis, N.; Cookson, D.; Balsara, N. P. *Macromolecules* **2007**, *40*, 4578−4585.
(20) Young, W. S.; Epps, T. H. *Macromolecules* **2012**, *45*, 4689−4697.
(21) Teran, A. A.; Mullin, S. A.; Hallinan, D. T.; Balsara, N. P. *ACS Macro Lett.* **2012**, *1*, 305−309.
(22) Jo, G.; Ahn, H.; Park, M. J. *ACS Macro Lett.* **2013**, *2*, 990−995.
(23) Hallinan, D. T.; Mullin, S. A.; Stone, G. M.; Balsara, N. P. *J. Electrochem. Soc.* **2013**, *160*, A464−A470.
(24) Yuan, R.; Teran, A. A.; Gurevitch, I.; Mullin, S. A.; Wanakule, N. S.; Balsara, N. P. *Macromolecules* **2013**, *46*, 914−921.
(25) Nakamura, I.; Balsara, N. P.; Wang, Z. G. *ACS Macro Lett.* **2013**, *2*, 478−481.
(26) Schulze, M. W.; McIntosh, L. D.; Hillmyer, M. A.; Lodge, T. P. *Nano Lett.* **2014**, *14*, 122−126.
(27) Sun, J.; Liao, X.; Minor, A. M.; Balsara, N. P.; Zuckermann, R. N. *J. Am. Chem. Soc.* **2014**, *136*, 14990−14997.
(28) Gomez, E. D.; Panday, A.; Feng, E. H.; Chen, V.; Stone, G. M.; Minor, A. M.; Kisielowski, C.; Downing, K. H.; Borodin, O.; Smith, G. D. *Nano Lett.* **2009**, *9*, 1212−1216.
(29) Morita, M.; Fukumasa, T.; Motoda, M.; Tsutsumi, H.; Matsuda, Y.; Takahashi, T.; Ashitaka, H. J. *Electrochem. Soc.* **1990**, *137*, 3401−3404.
(30) Doyle, M.; Fuller, T. F.; Newman, J. *Electrochim. Acta* **1994**, *39*, 2073−2081.
(31) Fragiadakis, D.; Dou, S.; Colby, R. H.; Runt, J. *J. Chem. Phys.* **2009**, *130*, 064907.
(32) Liang, S.; Choi, U. H.; Liu, W.; Runt, J.; Colby, R. H. *Chem. Mater.* **2012**, *24*, 2316−2323.
(33) Bouchet, R.; Maria, S.; Meziane, R.; Aboulaich, A.; Lienafa, L.; Bonnet, J. P.; Armand, M. *Nat. Mater.* **2013**, *12*, 452−457.
(34) Feng, S.; Shi, D.; Liu, F.; Zheng, L.; Nie, J.; Feng, W.; Huang, X.; Armand, M.; Zhou, Z. *Electrochim. Acta* **2013**, *93*, 254−263.
(35) Inceoglu, S.; Rojas, A. A.; Devaux, D.; Chen, X. C.; Stone, G. M.; Balsara, N. P. *ACS Macro Lett.* **2014**, *3*, 510−514.
(36) Kim, O.; Kim, S. Y.; Ahn, H.; Kim, C. W.; Rhee, Y. M.; Park, M. J. *Macromolecules* **2012**, *45*, 8702−8713.
(37) Sax, J.; Ottino, J. M. *Polym. Eng. Sci.* **1983**, *23* (3), 165−176.
(38) Volel, M.; Armand, M. *Macromolecules* **2004**, *37*, 8373−8380.
(39) Edman, L.; Doeff, M. M.; Ferry, A.; Kerr, J.; De Jonghe, L. C. *J. Phys. Chem. B* **2000**, *104*, 3476−3480.
(40) Doyle, M.; Newman, J. *J. Electrochem. Soc.* **1995**, *142*, 3465−3468.

DOI: 10.1021/mz500717j
ACS Macro Lett. 2015, 4, 225−230